
Training Dense Object Nets: A Novel Approach

Anonymous Author(s)

Affiliation

Address

email

Abstract

We present a novel framework for mining dense visual object descriptors produced by Dense Object Nets (DON) without explicitly training DON. DON’s dense visual object descriptors are robust to changes in viewpoint and configuration. However, training DON requires image pairs with correspondence mapping, which can be computationally expensive and limit the dimensionality and robustness of the descriptors, limiting object generalization. To overcome this, we propose a synthetic augmentation data generation procedure and a novel deep learning architecture that produces denser visual descriptors while consuming fewer computational resources. Furthermore, our framework does not require image-pair correspondence mapping and demonstrates its one of the applications as a robot-grasping pipeline. Experiments show that our approach produces descriptors as robust as DON.

1 Introduction

Creating a general-purpose robot capable of carrying out practical activities like Chappie [1] or C-3PO [2], is a long-standing objective of robotics and robotic manipulation. While advancements have been made recently in adjacent domains, achieving this goal remains a work in progress. For instance, AlphaGo [3], a game-playing artificial intelligence system trained entirely on self-play, defeated the world’s best human Go player at the time. Subsequently, Silver et al. [4] developed artificial intelligence algorithms that mastered the game of chess, Go, World of Warcraft [5], and Shogi, surpassing human playing expertise. Most of these algorithms learn directly from visual data such as gameplay recordings or online video streams, emphasizing the importance of visual data in AI. Meanwhile, the launch of AlexNet [6] in 2012 transformed the field of computer vision. Other visual tasks, such as semantic segmentation [7], object identification and recognition [8], and human pose estimation [9], have also witnessed significant gains in recent years. In robotics, significant breakthroughs have been made, ranging from self-driving cars to humanoid robots capable of performing complex tasks using cameras and other vision sensors. Despite these advancements, the most frequently used robotic manipulation systems have not evolved much in the previous 30 years. Typical auto-factory robots continue to perform repetitive operations such as welding and painting, with the robot following a pre-programmed course with no feedback from the surroundings. If we want to increase the utility of our robots, we must move away from highly controlled settings and robots that perform repetitive actions with little feedback or adaptability capabilities. Liberating ourselves from these constraints of controlled settings-based manufacturing would allow us to enter new markets, as witnessed by the proliferation of firms [10] competing in the logistics domain.

The ideal object representation for robot grasping and manipulation tasks remains to be engineered today. Existing representations may not be suitable for complex tasks due to limited capabilities of understanding an object’s geometrical and structural information. In 2018, Florence et al. [11] introduced a novel visual object representation to the robotics community, terming it “dense visual object descriptors”. DON, an artificial intelligence framework proposed by Florence et al. [11] produces dense visual object descriptors. In detail, the DON converts every pixel in the image

($I[u, v] \in \mathbb{R}^3$) to a higher dimensional embedding ($I_D[u, v] \in \mathbb{R}^D$) such that $D \in \mathbb{N}^+$ consuming image-pair correspondences as input yielding pixelwise embeddings which are nothing but dense local descriptors. The dense visual object descriptor generalizes an object up to a certain extent and has been recently applied to rope manipulation [12], block manipulation [13], robot control [14], fabric manipulation [15] and robot grasp pose estimation [16, 17]. Adrian et al. [17] further demonstrated that DON can be trained on synthetic data and still generalize to real-world objects. Furthermore, Adrian et al. [17] demonstrated that the quality of descriptors produced by the DON framework depends on the higher or longer embedding dimension. We tried training the DON on a computation device equipped with NVIDIA RTX A6000 GPU with 48GB VRAM. However, we could not train the DON to produce a higher embedding dimension due to the limited VRAM. The DON framework is computationally expensive, as shown in Table 1, and limits the user to generalize objects to a certain extent making it difficult to use as a robot grasping pipeline in real-world logistics and warehouse automation scenarios.

Table 1: Benchmark of DON framework trained on GPU with 48GB VRAM with 128 image-pair correspondences, batch size of 1 and “Pixelwise NTXENT Loss” [17] as a loss function.

GPU VRAM consumption to train DON				
Descriptor Dimension	3	8	16	32
VRAM Usage (GB)	9.377	13.717	20.479	30.067

To overcome the computation resource limitation to produce denser visual object descriptors, we propose a novel framework to train and extract dense visual object descriptors produced by DON, which is computationally efficient.

2 Related Work

We are solely interested in computing dense visual object descriptors of an object. The DON training strategy in [11] relies on the depth information for computing correspondences in an image pair using camera intrinsics and pose information [18]. However, when employing consumer-grade depth cameras for capturing the depth information, the depth cameras capture noisy depth in cases of tiny, reflecting objects, which are common in industrial environments. In the meantime, Kupcsik et al. [16] used Laplacian Eigenmaps [19] to embed a 3D object model into an optimally generated embedding space acting as a target to train DON in a supervised fashion. The optimal embeddings brings in more domain knowledge by associating 3D object model to images views. Kupcsik et al. [16] efficiently apply it to smaller, texture-less and reflective objects by eliminating the need of the depth information. Kupcsik et al. [16] further compare training strategies for producing 6D grasps for industrial objects and show that a unique supervised training approach increases pick-and-place resilience in industry-relevant tasks.

Florence [20] has found that the pixelwise contrastive loss function used to train DON might not perform well if a computed correspondence is spatially inconsistent (analogously to the case of noisy depth information). This further highlights that the precision of contrastive-trained models can be sensitive to the relative weighting between positive-negative sampled pixels. Instead, the Florence [20] introduces a new continuous sampling-based loss function called “Pixelwise Distribution Loss”. The pixelwise distribution loss is much more effective as it is a smooth continuous pixel space sampling method compared to the discrete pixel space sampling method based on pixelwise contrastive loss. The pixelwise distribution loss regresses a set of probability distribution heatmaps aiming to minimize the divergence between the predicted heatmap and the ground truth heatmap mitigating errors in correspondences. Furthermore, the pixelwise distribution loss does not need non-matching correspondences compared to the pixelwise contrastive loss. Differently, Hadjivelichkov and Kanoulas [21] extends the DON training using semantic correspondences between objects in multi-object or cluttered scenes overcoming the limitations of [18, 19]. The authors, Hadjivelichkov and Kanoulas [21] employ offline unsupervised clustering based on confidence in object similarities to generate hard and soft correspondence labels. The computed hard and soft labels lead DON in learning class-aware dense object descriptors, introducing hard and soft margin constraints in the proposed pixelwise contrastive loss to train DON. Further eliminating the need for camera pose and intrinsic information along with depth information to compute correspondences in an image

pair, Yen-Chen et al. [22] used NeRF [23] to train DON. The NeRF [23] recreates a 3D scene from a sequence of images captured by the smartphone camera. The correspondences are extracted from the synthetically reconstructed scene to train DON. Recently, based on SIMCLR inspired frameworks [24, 25], Adrian et al. [17] introduced similar architecture and another novel loss function called “Pixelwise NT-Xent loss” to train DON more robustly. The pixelwise nt-xent loss consumes synthetic correspondences independent of depth cameras computed from image augmentations to train DON. Adrian et al.’s experiments show that the novel loss function is invariant with respect to the batch size. Additionally adopted “ $PCK@k$ ” metric has been adopted as in proceedings [26, 27] to evaluate and benchmark DON on cluttered scenes previously not benchmarked.

In the proposed framework we do not use any loss functions in [11, 20, 16, 17, 21, 22] to train DON however we adopt the network architecture from [11] and train on the task of the “KeypointNet”[28] with adaption of the loss functions proposed in [28, 29].

3 Methodology

3.1 DNN Framework and Mining Methodology

As a backbone, we employ ResNet-34 architecture [30]. We preserve the last dense feature layer in the ResNet-34 DNN and remove the last flatten method and linear layer that is popularly used for image classification tasks. The backbone downsamples the RGB image $I_{RGB} \in \mathbb{R}^{H \times W \times 3}$ to dense features $I_d \in \mathbb{R}^{h \times w \times D}$ such that $h \ll H, w \ll W$ and $D \in \mathbb{N}^+$. We directly upsample the dense features from the identity layer as illustrated in the Figure 1 in page 3 as follows:

$$f_U : I \in \mathbb{R}^{h \times w \times D} \rightarrow I_D \in \mathbb{R}^{H \times W \times D}, \quad (1)$$

the upsampled dense features substitutes as dense visual local descriptors produced from the DON. Similarly as in [28], we stack spatial-probability regressing layer and depth regressing layer on top of the identity layer to predict $N \in \mathbb{N}^+$ number of keypoint’s spatial-probability as follows:

$$f_S : I_d \in \mathbb{R}^{h \times w \times D} \rightarrow I_s^N \in \mathbb{R}^{h \times w \times N}, \text{ such that } \sum_h \sum_w I_s^N = 1.0^N, \quad (2)$$

and depth as follows:

$$f_D : I_d \in \mathbb{R}^{h \times w \times D} \rightarrow I_d^N \in \mathbb{R}^{h \times w \times N}. \quad (3)$$

We incorporate continuous sampling method f_E from [20, 28] to convert the upsampled predicted spatial-probability and depth of a keypoint to spatial-depth expectation as follows:

$$f_E \circ g_E : [I_s, I_d] \rightarrow [u, v, d]^T \in \mathbb{R}^3, \text{ where } g_E : I \in \mathbb{R}^{h \times w \times N} \rightarrow I \in \mathbb{R}^{H \times W \times N}. \quad (4)$$

Furthermore, we train the DNN in a twin architecture fashion as depicted in the Figure 2 in page 4 as proposed in [24, 25, 11, 20, 16, 17, 21, 22] on the KeypointNet task.

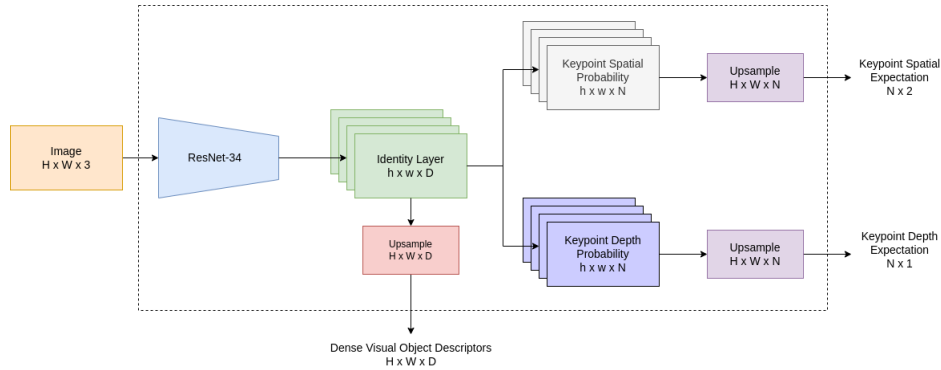


Figure 1: Illustration of novel DNN architecture designed to efficiently compute and seamlessly extract dense visual object descriptors. During inference we extract dense visual object descriptors directly from the network and ignore predicted spatial-depth expectation of the keypoints.

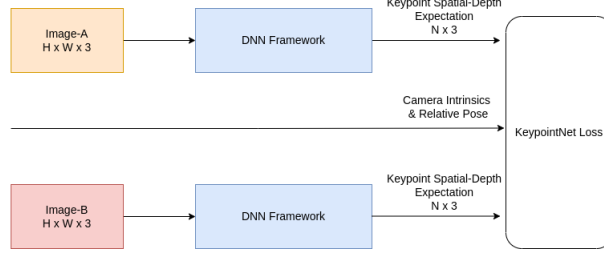


Figure 2: Depiction of twin DNN architecture’s training strategy.

3.2 Loss Function Modifications

For training, we directly adopt silhouette consistency loss (\mathcal{L}_{obj}), variance loss (\mathcal{L}_{var}) and separation loss (\mathcal{L}_{sep}) functions from [28] to train the network on the keypoint prediction task. However, we modify the multi-view consistent loss and relative pose estimation loss. In the case of multi-view consistency loss we project the predicted spatial-depth expectation using camera intrinsics as follows:

$$X_{cam} \in \mathbb{R}^{3 \times 1} = \mathcal{I}_{cam}^{-1} [u, v, 1.0]^T \otimes d, \text{ where } \mathcal{I}_{cam} \in \mathbb{R}^{3 \times 3} \text{ and } u, v, d \in \mathbb{R}^+. \quad (5)$$

Furthermore, we project the camera coordinates of the keypoints regressed on both images to the world coordinates using camera transformation and compute Huber Loss [31] represented as \mathcal{H} in Equation 6 as multi-view consistency loss as follows:

$$\mathcal{L}_{mvc} \in \mathbb{R} = \mathcal{H}(\mathcal{T}_{C \rightarrow W}^A \hat{X}_{cam}^A, \mathcal{T}_{C \rightarrow W}^B \hat{X}_{cam}^B), \text{ where } \mathcal{T}_{C \rightarrow W} \in SE(3) \text{ and } \hat{X}_{cam} = [X_{cam}, 1.0]^T \in \mathbb{R}^{4 \times 1}, \quad (6)$$

this modification is geometrically more intuitive as all the keypoints projected from different camera viewpoints into world coordinates occupy the same value additionally, using Huber Loss creates smoother gradients to optimize the DNN compared to the original implementation of Euclidean distance. In Equation 6 $SE(3) \in \mathbb{R}^{4 \times 4}$ is a “Special Euclidean Group” [32]. We do not discard the relative transformation information to calculate the relative pose loss as suggested in [28] and being influenced from [29] we modified the relative pose loss as follows:

$$\mathcal{L}_{pose} = \|\log(\mathcal{T}_{truth}^\dagger \mathcal{T}_{pred})\|, \text{ where } \log : SE(3) \rightarrow \mathfrak{se}(3) \text{ and } \mathcal{T}^\dagger = \begin{bmatrix} R^T & -R^T t \\ 0^T & 1 \end{bmatrix} \in SE(3). \quad (7)$$

3.3 Controlled Dataset Engineering

We have chosen the cap object for creating synthetic dataset as the cap mesh models are readily available in the “Shapenet” library [33] as it possess rich object information including textures. Blenderproc [34] is used to generate the synthetic cap dataset by using of the 10 number of cap models from [33] library. Furthermore, the caps are chosen such that each of them have distinct shapes, designs and colors. For this controlled dataset, 100 random cameras are added in the environment with random poses capturing depth, camera extrinsics information (referring to $\mathcal{T}_{C \rightarrow W}$ in Equation 6) and object mask for each viewpoint for each cap model. To make the training more robust such that networks are more object-centric, the images are additionally augmented with random backgrounds and noisy backgrounds as depicted in Figure 3 in page 5 in addition to the color jitter and greyscale augmentations. For color jitter and greyscale augmentation we use available “Torchvision” [35] library.

References

- [1] N. Blomkamp, H. Zimmer, and S. Kinberg. *Chappie*. Sony Pictures Home Entertainment, 2015.
- [2] G. Lucas and S. Ulstein. *Star wars*. 20th Century-Fox, 1977.
- [3] D. Silver, T. Hubert, J. Schrittwieser, I. Antonoglou, M. Lai, A. Guez, M. Lanctot, L. Sifre, D. Kumaran, T. Graepel, et al. “A general reinforcement learning algorithm that masters chess, shogi, and Go through self-play”. In: *Science* 362.6419 (2018), pp. 1140–1144.

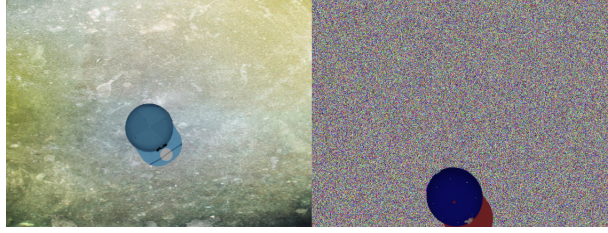


Figure 3: The image in the right illustrates the noisy background augmentation and the image in left depicts random background augmentation.

- 147 [4] D. Silver, A. Huang, C. J. Maddison, A. Guez, L. Sifre, G. Van Den Driessche, J. Schrittwieser, I.
148 Antonoglou, V. Panneershelvam, M. Lanctot, et al. “Mastering the game of Go with deep neural networks
149 and tree search”. In: *nature* 529.7587 (2016), pp. 484–489.
- 150 [5] B. Entertainment. *World of warcraft*. Insight Editions, Division Of Palac, 2013.
- 151 [6] A. Krizhevsky, I. Sutskever, and G. E. Hinton. “Imagenet classification with deep convolutional neural
152 networks”. In: *Communications of the ACM* 60.6 (2017), pp. 84–90.
- 153 [7] J. Long, E. Shelhamer, and T. Darrell. “Fully convolutional networks for semantic segmentation”. In:
154 *Proceedings of the IEEE conference on computer vision and pattern recognition*. 2015, pp. 3431–3440.
- 155 [8] K. He, G. Gkioxari, P. Dollár, and R. Girshick. “Mask r-cnn”. In: *Proceedings of the IEEE international
156 conference on computer vision*. 2017, pp. 2961–2969.
- 157 [9] R. A. Güler, N. Neverova, and I. Kokkinos. “Densepose: Dense human pose estimation in the wild”. In:
158 *Proceedings of the IEEE conference on computer vision and pattern recognition*. 2018, pp. 7297–7306.
- 159 [10] sereact. “AI Robots for Production. Today”. <https://sereact.ai/en>.
- 160 [11] P. R. Florence, L. Manuelli, and R. Tedrake. “Dense object nets: Learning dense visual object descriptors
161 by and for robotic manipulation”. In: *arXiv preprint arXiv:1806.08756* (2018).
- 162 [12] P. Sundaresan, J. Grannen, B. Thananjeyan, A. Balakrishna, M. Laskey, K. Stone, J. E. Gonzalez, and K.
163 Goldberg. “Learning Rope Manipulation Policies Using Dense Object Descriptors Trained on Synthetic
164 Depth Data”. In: *CoRR* abs/2003.01835 (2020). arXiv: 2003.01835.
- 165 [13] C.-Y. Chai, K.-F. Hsu, and S.-L. Tsao. “Multi-step Pick-and-Place Tasks Using Object-centric Dense
166 Correspondences”. In: *2019 IEEE/RSJ International Conference on Intelligent Robots and Systems
167 (IROS)*. 2019, pp. 4004–4011. DOI: 10.1109/IR0S40897.2019.8968294.
- 168 [14] P. Florence, L. Manuelli, and R. Tedrake. “Self-supervised correspondence in visuomotor policy learning”.
169 In: *IEEE Robotics and Automation Letters* 5.2 (2019), pp. 492–499.
- 170 [15] A. Ganapathi et al. “Learning Dense Visual Correspondences in Simulation to Smooth and Fold Real
171 Fabrics”. In: *2021 IEEE International Conference on Robotics and Automation (ICRA)*. 2021, pp. 11515–
172 11522. DOI: 10.1109/ICRA48506.2021.9561980.
- 173 [16] A. Kupcsik, M. Spies, A. Klein, M. Todescato, N. Waniek, P. Schillinger, and M. Bürger. “Supervised
174 Training of Dense Object Nets using Optimal Descriptors for Industrial Robotic Applications”. In: *arXiv
175 preprint arXiv:2102.08096* (2021).
- 176 [17] D. B. Adrian, A. G. Kupcsik, M. Spies, and H. Neumann. “Efficient and Robust Training of Dense
177 Object Nets for Multi-Object Robot Manipulation”. In: *2022 International Conference on Robotics and
178 Automation (ICRA)*. IEEE. 2022, pp. 1562–1568.
- 179 [18] R. Hartley and A. Zisserman. *Multiple view geometry in computer vision*. Cambridge university press,
180 2003.
- 181 [19] M. Belkin and P. Niyogi. “Laplacian eigenmaps for dimensionality reduction and data representation”. In:
182 *Neural computation* 15.6 (2003), pp. 1373–1396.
- 183 [20] P. R. Florence. “Dense visual learning for robot manipulation”. PhD thesis. Massachusetts Institute of
184 Technology, 2020.
- 185 [21] D. Hadjivelichkov and D. Kanoulas. “Fully Self-Supervised Class Awareness in Dense Object Descrip-
186 tors”. In: *5th Annual Conference on Robot Learning*. 2021.
- 187 [22] L. Yen-Chen, P. Florence, J. T. Barron, T.-Y. Lin, A. Rodriguez, and P. Isola. *NeRF-Supervision: Learning
188 Dense Object Descriptors from Neural Radiance Fields*. 2022. DOI: 10.48550/ARXIV.2203.01913.
- 189 [23] B. Mildenhall, P. P. Srinivasan, M. Tancik, J. T. Barron, R. Ramamoorthi, and R. Ng. “Nerf: Representing
190 scenes as neural radiance fields for view synthesis”. In: *Communications of the ACM* 65.1 (2021), pp. 99–
191 106.
- 192 [24] T. Chen, S. Kornblith, M. Norouzi, and G. Hinton. “A simple framework for contrastive learning of visual
193 representations”. In: *International conference on machine learning*. PMLR. 2020, pp. 1597–1607.

- 194 [25] J. Zbontar, L. Jing, I. Misra, Y. LeCun, and S. Deny. “Barlow twins: Self-supervised learning via
195 redundancy reduction”. In: *International Conference on Machine Learning*. PMLR. 2021, pp. 12310–
196 12320.
- 197 [26] C.-Y. Chai, K.-F. Hsu, and S.-L. Tsao. “Multi-step pick-and-place tasks using object-centric dense
198 correspondences”. In: *2019 IEEE/RSJ International Conference on Intelligent Robots and Systems (IROS)*.
199 IEEE. 2019, pp. 4004–4011.
- 200 [27] M. E. Fathy, Q.-H. Tran, M. Z. Zia, P. Vernaza, and M. Chandraker. “Hierarchical metric learning and
201 matching for 2d and 3d geometric correspondences”. In: *Proceedings of the european conference on*
202 *computer vision (ECCV)*. 2018, pp. 803–819.
- 203 [28] S. Suwajanakorn, N. Snavely, J. J. Tompson, and M. Norouzi. “Discovery of latent 3d keypoints via
204 end-to-end geometric reasoning”. In: *Advances in neural information processing systems* 31 (2018).
- 205 [29] W. Zhao, S. Zhang, Z. Guan, W. Zhao, J. Peng, and J. Fan. “Learning deep network for detecting 3d
206 object keypoints and 6d poses”. In: *Proceedings of the IEEE/CVF Conference on computer vision and*
207 *pattern recognition*. 2020, pp. 14134–14142.
- 208 [30] K. He, X. Zhang, S. Ren, and J. Sun. “Deep residual learning for image recognition”. In: (2016), pp. 770–
209 778.
- 210 [31] P. J. Huber. “Robust estimation of a location parameter”. In: *Breakthroughs in statistics: Methodology*
211 *and distribution* (1992), pp. 492–518.
- 212 [32] W. P. Thurston. “Three-Dimensional Geometry and Topology, Volume 1”. In: *Three-Dimensional Geome-*
213 *try and Topology, Volume 1*. Princeton university press, 2014.
- 214 [33] A. X. Chang, T. Funkhouser, L. Guibas, P. Hanrahan, Q. Huang, Z. Li, S. Savarese, M. Savva, S. Song,
215 H. Su, et al. “Shapenet: An information-rich 3d model repository”. In: *arXiv preprint arXiv:1512.03012*
216 (2015).
- 217 [34] M. Denninger, M. Sundermeyer, D. Winkelbauer, Y. Zidan, D. Olefir, M. Elbadrawy, A. Lodhi, and
218 H. Katam. “Blenderproc”. In: *arXiv preprint arXiv:1911.01911* (2019).
- 219 [35] S. Marcel and Y. Rodriguez. “Torchvision the machine-vision package of torch”. In: *Proceedings of the*
220 *18th ACM international conference on Multimedia*. 2010, pp. 1485–1488.